Olami-Feder-Christensen model with quenched disorder

Manuel Bach, Felix Wissel, and Barbara Drossel
Institut für Festkörperphysik, TU Darmstadt, Hochschulstraße 6, 64289 Darmstadt, Germany
(Received 10 October 2007; revised manuscript received 25 April 2008; published 26 June 2008)

We study the Olami-Feder-Christensen model with quenched disorder in the coupling parameter α. In contrast to an earlier study by Mousseau [Phys. Rev. Lett. **77**, 968 (1996)], we do not find a phase diagram with several phase transitions, but continuous crossovers from one type of behavior to another. The crossover behavior is determined by the ratio of three length scales, which are the system size, the penetration depth of the boundary layer, and the correlation length introduced by the disorder.

DOI: 10.1103/PhysRevE.77.067101 PACS number(s): 05.65.+b, 45.70.Ht

The Olami-Feder-Christensen (OFC) earthquake model [1] is the prime example for a supposedly self-organized critical yet nonconservative model. Systems are said to be self-organized critical (SOC) if they are slowly driven and have avalanchelike dissipation events, the size distribution of which is a power law. An important characteristic of the OFC model is that the degree of dissipation can be tuned continuously by changing the coupling parameter α. Despite the simplicity of its dynamical rules, the OFC model shows a variety of interesting features that are unknown in equilibrium physics and appear to be crucial for generating the apparent critical (or almost critical) behavior. Among these features are a marginal synchronization of neighboring sites driven by the open boundary conditions [2], and a qualitative difference between system-wide earthquakes and smaller earthquakes [3]. The OFC model can easily be modified, and several versions with slightly different updating rules exist, which are also relevant for other fields of research [4,5]. Small changes in the model rules, such as replacing open boundary conditions with periodic boundary conditions [6], destroy the SOC behavior.

The OFC model originated by a simplification of the spring-block model by Burridge and Knopoff [7]. To each site of a square lattice we assign a continuous variable $z_{ij} \in [0,1]$ that represents the local energy. Starting with a random initial configuration taken from a flat distribution, the value z of all sites is increased at a uniform rate until a site ij reaches the threshold value $z_t=1$. This site is then said to topple, which means that the site is reset to zero and an energy αz_{ij} is passed to every nearest neighbor. If this causes a neighbor to exceed the threshold, the neighbor topples also, and the avalanche continues until all $z_{kl}<1$. Then the uniform increase resumes. The number of topplings defines the size s of an avalanche or "earthquake." The coupling parameter α can take on values in (0,0.25). Smaller α means more dissipation, and $\alpha=0.25$ corresponds to the conservative case. α is the only parameter of the model, apart from the system size L, the edge length of the square lattice. Except for the initial condition, the model is deterministic. The model has open boundary conditions, i.e., sites at the boundary receive energy only from three or two neighbors and topple therefore on average less often than sites in the interior, which leads to the formation of "patches" of sites with a similar energy. This patch formation proceeds from the boundaries inward [2,8]. There has been no agreement in the literature as to whether the model is indeed critical for all values of the coupling or only in the conservative case [9–11]. Due to the dynamics of the model, there occur avalanches of all sizes; the mechanisms producing these avalanches are different on different scales, though. Large avalanches are mainly patch-wide avalanches, while smaller avalanches occur within patches and constitute a series of foreshocks or aftershocks [12]. Also, avalanches at different distance from the boundaries have different sizes. A thorough numerical and analytical study in [13] showed finally that the observed "power laws" are *dirty* power laws, which appear like power laws over a wide range of parameters and over a few decades of avalanche sizes, while the "true" analytical form is no power law.

In this paper, we consider the effect of noise on the OFC model. In one of the first publications on the OFC model, it was found that the addition of small random energy packages to every toppled site does not change the exponents or the cutoff of the distributions [1]. In contrast, quenched disorder in the threshold values destroys criticality, changing the size distribution of avalanches to an exponentially decaying function [14]. It was concluded that disorder introduces a second length scale in the system, apart from the system size. Ceva addressed the stability against small lattice defects by changing the coupling locally to $\alpha_d \neq \alpha$ for some sites. For not too many defects, criticality appeared to be preserved, and the obtained power laws interpolate between the corresponding undisturbed systems [15,16]. Quenched disorder in the coupling constant at all sites was discussed in [17], which is the version we discuss in the following.

To each site ij, we assign a value $\alpha_{ij}=\alpha+\delta_{ij}$ with δ_{ij} being a random number chosen from the interval $[-\delta,\delta]$. Thus, the model now contains a second parameter δ. Mousseau [17], who introduced this version of the OFC model, found that for small (but not too small) values of δ, the entire system synchronizes, apart from a very narrow boundary layer. This separation leads to only small and system-wide avalanches. For larger values of δ, the avalanche-size distribution looks again like a power law, while for even larger noise the avalanche-size distribution decays exponentially. The parameter regions where these four "phases" (which we call more appropriately "regions") are found are indicated in the phase diagram, Fig. 1. Mousseau found that the transition from SOC to synchronization (from I to II) and back to SOC (from II to III) is relatively sharp, while the last transition (from III to IV) is smooth.

We will argue in the following that all the apparent phase

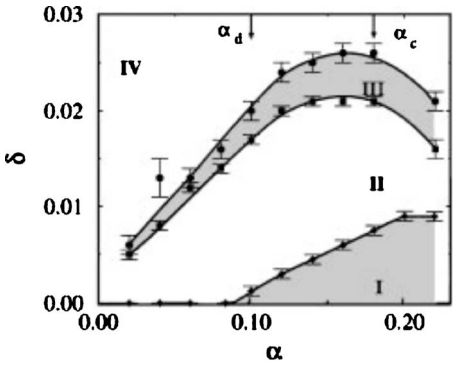

FIG. 1. Phase diagram as presented in [17]. Figure courtesy of N. Mousseau.

transitions are in fact smooth transitions due to the fact that the relative size of three different relevant scales changes as the parameters change. We begin by discussing the dependence of the avalanche-size distribution on the strength of the disorder, on the system size, and on the boundary conditions. We used the efficient algorithm introduced in [13], which implies that we can study only system sizes L that are a power of 2. If not stated otherwise, the parameters L and α are 64 and 0.11, so that increasing δ from 0.002 to 0.03 leads us to all four regions in the phase diagram by Mousseau (see Fig. 1).

Figure 2 shows the avalanche-size distribution for fixed $\alpha=0.11$ and varying δ. For $\delta=0.002$, the size distribution resembles a power law, which is characteristic of the SOC regime, but it has a small peak for large s, which indicates the beginning of the transition to synchronization. The next three curves (for $0.004 \leq \delta \leq 0.016$) contain only small avalanches and avalanches of the order of the system size, and they belong therefore to region II. For $\delta=0.018$ and 0.022, there appears to be again a power law (region III), while for even larger δ the avalanche-size distribution decays rapidly, and the system is therefore in region IV. All three transitions thus occur at the parameter values indicated in the phase diagram Fig. 1. The system size chosen in our simulations ($L=64$) is not far from that chosen by Mousseau ($L=50$).

Next, we point out that the transitions between the different regions depend on the system size. Mousseau found already that the boundary between the SOC and the synchronized phase (between I an II) moves downward in the phase diagram with increasing system size. Figure 3 (left) shows that the transitions between regions II, III, and IV must also

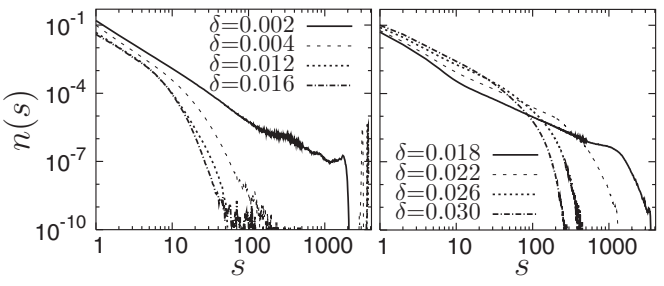

FIG. 2. Normalized size distribution of avalanches for $L=64$, $\alpha=0.11$, and different values of δ.

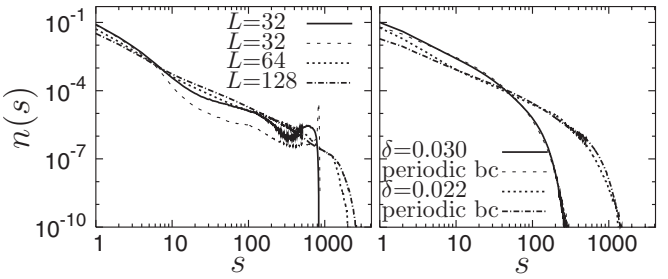

FIG. 3. (Left) Transition from one type of size distribution of avalanches to another type with increasing system size. Parameters are fixed at $(\alpha,\delta)=(0.11,0.020)$. For $L=32$, two simulations were performed. (Right) Size distribution of avalanches for $L=64$, $\alpha=0.11$, for two different values of δ, with open and periodic boundary conditions (BCs).

move downward with increasing system size. As L is increased for fixed α and δ, the shape of the curves changes from that of region II to that of regions III and IV: The first curves ($L=32$) are characteristic of region II (close to the boundary to I). The other curves ($L=64$ and 128) show the shape characteristic of regions III and IV. The cutoff hardly increases from $L=64$ to 128, indicating that the avalanches become less dependent on the system size when L is larger. We found generally that deep in region IV the avalanche-size distribution does not change at all when the system size is increased further. If the transitions between the different regions were conventional phase transitions, they would depend only on the parameters α and δ, but not on the system size (apart from the usual finite-size effects). Our simulation results therefore suggest that the transitions between the different regions are not real phase transitions but smooth crossovers, as the ratio between the system size and other characteristic lengths changes.

In addition to the dependence on the system size, there is also a dependence on the boundary conditions in some of the regions. It has been known for a long time that a SOC system (i.e., $\delta=0$) with periodic boundary conditions has only single topplings after a transient time [6], while the standard model (with open boundary conditions) shows the familiar power laws. In region II, a system with periodic boundary conditions shows only system-wide avalanches and no small avalanches [17]. In contrast, the avalanche-size distributions in regions III and IV are independent of the boundary conditions [see Fig. 3 (right)]. Together with the findings presented in the previous paragraph, we conclude that the boundary conditions affect only regions I and II, while the system size affects regions I–III. The avalanche-size distributions in region IV depend neither on the system size nor on the boundary conditions.

Before interpreting these findings further, we show snapshots of the model in the four regions (see Fig. 4). The first picture is taken in region I and is very similar to systems without disorder, with patches of different sizes and with the patch size increasing with increasing distance from the boundaries. However, the inner patches are larger than in the absence of disorder. In the second picture (region II), the boundary layer has become very small, and the inner part is synchronized. By watching the running simulation on the

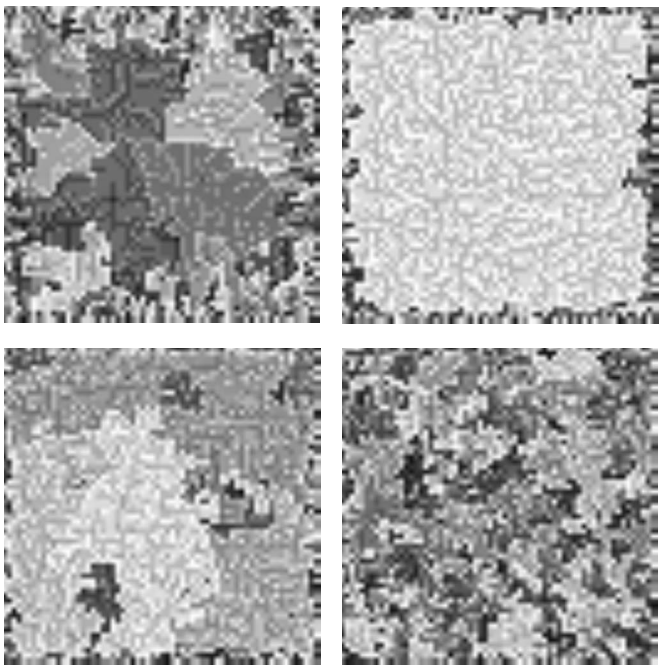

FIG. 4. Snapshots of systems in the stationary state for $L=64$ and $\alpha=0.11$. The disorder strength δ is 0.002 and 0.01 (top row) and 0.018 and 0.03 (bottom row).

computer screen, one can see that all sites in the inner part topple during the same avalanches. In the third and fourth pictures (regions III and IV), there is a very small boundary layer surrounding a pattern of patches of some characteristic size. In contrast to the first picture, the patch size does not increase with the distance from the boundary. Monitoring the system during the transient time, one realizes that the patches in region I are formed starting at the boundary, while the patches in region IV are formed everywhere at the same time.

These observations, together with the findings mentioned above, lead us to the following interpretation of the behavior of the model. There appear to be two characteristic length scales (apart from the system size). The first length scale is the thickness d of the boundary layer. The boundary layer is the region where patches are formed from the boundary inward, in the same way as in the model without randomness. This patch formation is due to the fact that sites at different distance from the boundary topple a different number of times, because sites closer to the boundary receive on average less energy due to the open boundary conditions. The smaller the toppling difference becomes (i.e., the farther away from the boundary a site is), the larger are the patches. Clearly, this process can continue only as long as the influence of the boundary on differences in the received energy is larger than the influence of the quenched randomness. In region I, this boundary layer spans the entire system, as confirmed by the snapshots and by the fact that a system with periodic boundary conditions has only very small avalanches and no patchy structure. In region II, the boundary layer is small, indicated not only by the snapshot but also by the fact that the small avalanches vanish in a system with periodic boundary conditions, which is fully synchronized. The transition from region I to II is thus accompanied by a decrease of the thickness of the boundary layer from system size to a value much smaller than the system size.

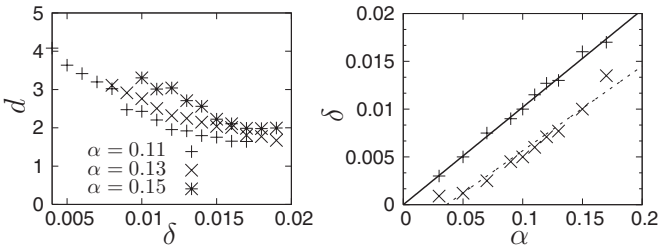

FIG. 5. Data for the boundary layer thickness d. Left: d as a function of δ for different α. Right: Parameter combinations for which $d=2$ or 3.5, indicated by + and $\times$, respectively. The solid lines are linear fits.

The second length scale is related to patches in the inner part of the system. For large noise, the exponential decay of the avalanche size distribution indicates that the randomness introduces a characteristic length scale ξ into the system, which is the typical extension of the largest avalanches. Since the sites affected by an avalanche form a patch with similar energy values, ξ is also related to the extension of patches. If we assume that there exists also such a characteristic scale for smaller randomness (which may be much larger than the system size), we can understand the transitions from region II to III and from III to IV: In region II, randomness is so small that $L<\xi$. Thus, only one large patch is visible in the inner part of the system. In region III, we have $L\approx\xi$; several (but not too many) patches are visible, and the cutoff of the avalanche size appears to be of the order of the system size. In region IV, we have $\xi\ll L$, and the characteristic patch size is clearly visible.

We evaluated d and ξ for those parameter regions, where these length scales are clearly visible. The thickness d of the boundary layer was evaluated on the basis of our observation that the size $s_{\max}$ of the largest avalanche is the size of the inner part of the system. Such an analysis is limited to parameter values deep in region II, where the inner part is so large that the avalanche size distribution splits nicely into a part for the small avalanches and a sharp peak at $s_{\max}$. Thus, d can be approximated by

$$d \simeq \frac{L^2 - s_{\max}}{4(L-1)}. \tag{1}$$

The simulation results for d are shown in Fig. 5. The left graph shows the values d obtained as function of δ for different α. As can be expected, d increases with increasing α and decreasing δ. The right graph shows those values of α and δ that lead to the same thickness $d=2$ or 3.5 of the boundary layer. Also shown is a linear fit, but in particular the curve for $d=3.5$ could also be fitted by a power law with a larger exponent. The curve becomes flatter with increasing d and moves to the right. We can therefore interpret the boundary between regions I and II in Fig. 1 as the line in parameter space where d assumes a fixed value somewhat larger than 3.5. In principle, d could also be evaluated for parameter values closer to the boundary to region I or III. For

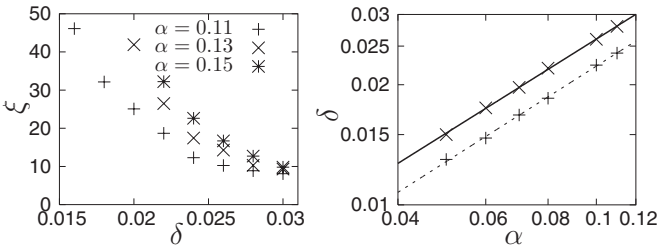

FIG. 6. Left: ξ as a function of δ for different α. Right: Parameter values α and δ that lead to the same avalanche-size distribution. Two different distributions indicated by + and × have been chosen. The solid (dashed) lines are power-law fits with an exponent 0.783 (0.795).

that purpose, one would have to evaluate the difference between systems with open and periodic boundary conditions in a more sophisticated way. This could be done by evaluating avalanche-size distributions and/or patch sizes as function of the distance from the boundary, and determining the distance d beyond which the difference between the distributions obtained for the two boundary conditions becomes smaller than some threshold.

When evaluating ξ, we focused on region IV. We determined ξ by the formula

$$\xi = \left(\frac{\int n(s) s^{10} ds}{\int n(s) ds} \right)^{1/20}. \quad (2)$$

By evaluating the tenth moment of the avalanche-size distribution, we obtain a good estimate of the largest avalanche size; use of other high moments gives similar results. We compared for some examples the value ξ^2 with the typical patch size estimated by counting pixels in the snapshots, and we found good agreement.

Figure 6 shows on the left our results for ξ as a function of δ for different α. By comparing these data to the avalanche-size distribution $n(s)$ for decreasing δ, we found that $n(s)$ starts developing a peak at values of δ such that $\xi \approx L/2$. This confirms our above phenomenological arguments that the transition between regions III and IV occurs when ξ is of the order of L. The right graph in Fig. 6 shows parameter combinations for which the avalanche-size distributions $n(s)$ agree with each other, which means that also the values ξ agree with each other. Lines of constant ξ appear to be a power law with an exponent 0.79 in the α-δ plane. However, this dependence $\delta \sim \alpha^{0.79}$ of lines with fixed ξ should not be extrapolated to small α, since δ would eventually become larger than α, which makes no sense. Our simulations did not explore that part of parameter space because simulations for small α and sufficiently large system sizes take extremely long.

To conclude, we have presented evidence that the "phase transitions" seen in the OFC model with quenched randomness are in fact smooth transitions between regions where the ratios between the system size, the boundary layer thickness d, and the noise-dependent correlation length ξ change. When d is of the order of the system size L, the model behaves similarly to one without randomness (region I); when $d \ll L \ll \xi$, almost the entire system is synchronized (region II); when $d \ll L \simeq \xi$, there occur avalanches of all sizes (region III); when $d \ll \xi \ll L$, the avalanche size distribution decays exponentially (region IV). Thus, randomness introduced two length scales into the model but no real phase transitions. Of course, there still remain some open questions. We have no proof that ξ cannot become infinite for some nonzero value of δ. Furthermore, we have not investigated what happens when δ becomes of the order of α or when α becomes very small.

This work was supported by the Deutsche Forschungsgemeinschaft (DFG) under Contracts No. Dr300/3-1 and No. Dr300/3-2.

[1] Z. Olami and S. Hans Jacob Feder, and K. Christensen, Phys. Rev. Lett. **68**, 1244 (1992).
[2] A. A. Middleton and C. Tang, Phys. Rev. Lett. **74**, 742 (1995).
[3] S. Lise and M. Paczuski, Phys. Rev. E **64**, 046111 (2001).
[4] J. E. S. Socolar, G. Grinstein, and C. Jayaprakash, Phys. Rev. E **47**, 2366 (1993).
[5] A. Corral, C. J. Pérez, A. Diaz-Guilera, and A. Arenas, Phys. Rev. Lett. **74**, 118 (1995).
[6] P. Grassberger, Phys. Rev. E **49**, 2436 (1994).
[7] R. Burridge and L. Knopoff, Bull. Seismol. Soc. Am. **57**, 341 (1967).
[8] B. Drossel, Phys. Rev. Lett. **89**, 238701 (2002).
[9] J. X. de Carvalho and C. P. C. Prado, Phys. Rev. Lett. **84**, 4006 (2000).
[10] J. X. de Carvalho and C. P. C. Prado, Phys. Rev. Lett. **87**, 039802 (2001).
[11] G. Miller and C. J. Boulter, Phys. Rev. E **66**, 016123 (2002).
[12] S. Hergarten and H. J. Neugebauer, Phys. Rev. Lett. **88**, 238501 (2002).
[13] F. Wissel and B. Drossel, Phys. Rev. E **74**, 066109 (2006).
[14] I. Jánosi and J. Kertész, Physica A **200**, 179 (1993).
[15] H. Ceva, Phys. Rev. E **52**, 154 (1995).
[16] H. Ceva, Phys. Lett. A **245**, 413 (1998).
[17] N. Mousseau, Phys. Rev. Lett. **77**, 968 (1996).